J. Plasma Fusion Res. SERIES, Vol. 5 (2002) 22–27

Recent Development of LHD Experiment

MOTOJIMA Osamu, YAMADA Hiroshi, ASHIKAWA Naoko, EMOTO Masahiko, FUNABA Hisamichi, GOTO Motoshi, IDA Katsumi, IDEI Hiroshi, IKEDA Katsunori, INAGAKI Shigeru, INOUE Noriyuki, ISOBE Mitsutaka, KANEKO Osamu, KAWAHATA Kazuo, KHLOPENKOV Konstantin, KOBUCHI Takashi, KOMORI Akio, KOSTRIOUKOV Artem, KUBO Shin, KUMAZAWA Ryuhei, LIANG Yunfeng, MASUZAKI Suguru, MINAMI Takashi, MIYAZAWA Junichi, MORISAKI Tomohiro, MORITA Shigeru, MURAKAMI Sadayoshi, MUTO Sadatsugu, MUTO Takashi, NAGAYAMA Yoshio, NAKAMURA Yukio, NAKANISHI Hideya, NARIHARA Kazumichi, NARUSHIMA Yoshiro, NISHIMURA Kiyohiko, NODA Nobuaki, NOTAKE Takashi, OHDACHI Satoshi, OHYABU Nobuyoshi, OKA Yoshihide, OSAKABE Masaki, OZAKI Tetsuo, PETERSON Byron, SAGARA Akio, SAITO Kenji, SAKAKIBARA Satoru, SAKAMOTO Ryuichi, SASAO Mamiko, SATO Kuninori, SATO Motoyasu, SEKI Tetsuo, SHIMOZUMA Takashi, SHOJI Mamoru, SUZUKI Hajime, TAKEIRI Yasuhiko, TANAKA Kenji, TAMURA Naoki, TOI Kazuo, TOKUZAWA Tokihiko, TORII Yuki, TSUMORI Katsuyoshi, WATANABE Kiyomasa, WATANABE Tsuguhiro, YAMADA Ichihiro, YAMOMOTO Satoshi, YOKOYAMA Masayuki, YOSHIMURA Yasuo, WATARI Tetsuo, XU Yuhoug, CHIKARAISHI Hirotaka, HAMAGUCHI Shinji, HISHINUMA Yoshimitsu, IMAGAWA Shinsaku, IWAMOTO Akifumi, MAEKAWA Ryuji, MITO Toshiyuki, NISHIMURA Arata, TAMURA Hitoshi, YAMADA Shuichi, YANAGI Nagato, TAKAHATA Kazuya, ITOH Kimitaka, MATSUOKA Keisuke, OHKUBO Kunizo, SATOW Takashi, SUDO Shigeru, UDA Tatsuhiko and YAMAZAKI Kozo

National Institute for Fusion Science, Toki 509-5292, Japan

(Received: 21 December 2001 / Accepted: 23 August 2002)

Abstract

Experiments in LHD have been developing steadily since the first plasma in 1998. Many encouraging physical achievements have emerged during five experimental campaigns. The most significant finding is that MHD stability and good transport are compatible in the inward shifted configuration. Within the range of beta up to 3% and the collisionality down to 0.05, the energy confinement keeps gyro-Bohm characteristics, and no significant degradation due to the neoclassical transport and MHD instabilities have not been observed. The present 5th experimental campaign with upgraded heating resources has realized the electron temperature exceeding 10 keV which shows a sign of an internal transport barrier and the ion temperature of 5 keV. Technology of large scale superconducting system has been demonstrated successfully.

Keywords:

LHD, heliotron, net current-free plasma, inward shifted configuration, internal transport barrier, long-pulse discharge, high beta, low collisionality

Corresponding author's e-mail: motojima@lhd.nifs.ac.jp

1. Introduction

The Large Helical Device (LHD) is a large heliotron type device employing a full superconducting magnet system. The nominal major and minor radii are 3.9 m and 0.6 m, respectively. Built-in divertor as well as superconducting coils boost an intrinsic advantage of net current-free plasmas to steady state operation [1-8]. The cross-section of LHD is illustrated in Fig. 1, and its device specifications and heating capability are listed in Table 1. It is the largest superconducting fusion experimental device. The major goal of the LHD experiment is to demonstrate high performance of helical plasmas in a reactor relevant plasma regime. Large dimension and strong magnetic field up to 3 T can realize plasmas with high performance in the absolute physical quantities and also enables exploration in extended regimes of non-dimensional physical parameters, i.e., low collisionality and high β. Plasma generation is normally initiated by ECRH and then the main power from NBI and/or ICH is added to heat the plasma. With good wall conditions, however, plasma initiation or start-up is possible by NBI alone [9]. This skillful scheme of start-up enables the operation independent of the ECRH resonance conditions and facilitates high-β study in a low magnetic field. In the first three and a half years of experiment, a lot of physical achievements and findings have been accumulated, which provide a new perspective of attractive fusion reactor of net current-free plasmas. Development of LHD experiments are reviewed with emphasis on the recent results from the 5th experimental campaign in 2001 in this article.

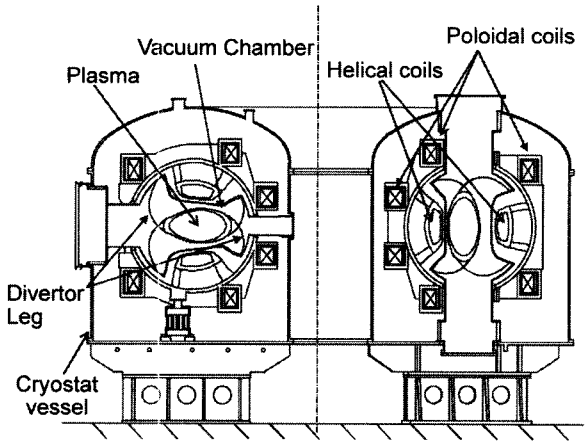

Fig. 1 Illustration of cross-section of the Large Helical Device (LHD)

Table 1 LHD device parameters and heating power used in the experiment.

Major radius	3.9 m	B_0	2.9 T
Coil minor radius	0.975 m	ι (0) / ι (a)	0.35 / 1.3
Plasma radius	~0.6 m	Heating Power (absorbed)	
l/m	2 / 10	NBI	8.5 MW
α (pitch modulation)	0.1	ECRH	1.7 MW
Helical ripple	0.2	ICRF	2.7 MW

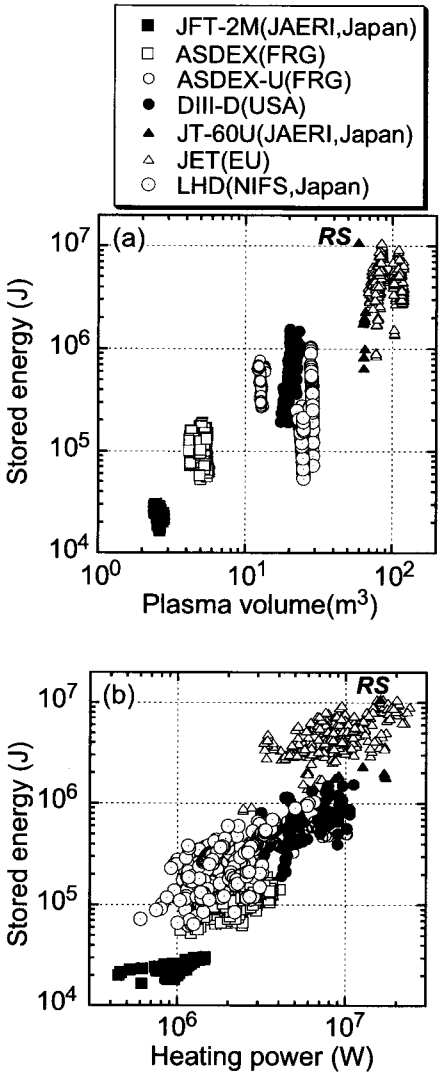

Fig. 2 Operational regime of major tokamaks and LHD. The stored energy as a function of (a) the plasma volume and (b) the heating power. The tokamak data is given by ITER Elmy-H mode database. RS denotes the highest performance in JT-60U with the reversed shear.

2. Development of Performance

The LHD experiment has begun in March 1998 after its eight-year construction. Four experimental campaigns have been conducted successfully and the 5th campaign is carried out in 2001. The total cryogenic operation time, coil excitations and plasma shots have exceeded 20000 hours, 500 times and 30000 shots, respectively. These experiences have demonstrated reliability and safety of the large scale superconducting system. The plasma parameters are continuously enhanced along the reinforcement of heating and particle controlling resources. Nowaday a plasma shot with several MW of heating power is available every 3 minutes. Achieved plasma parameters so far are listed in Table 2. Figure 2 shows the achieved stored energy as a function of a plasma volume and heating power with major tokamak experiments. The operation regime of LHD lies close to the major large tokamaks and is comparable to DIII-D and ASDEX-U. Recently high central electron temperature of 10 keV has been obtained by localizing ECRH power deposition (a total of 1.2 MW) at the magnetic axis (see Fig. 3). The geometrical optimization to minimize the neoclassical transport and well focused ray of ECRH have realized this high temperature.

Table 2 Achieved plasma parameters

	T	$\bar{n}_e$
High Electron Temperature	10 keV	6.0×10^{18}m^{-3}
High Ion Temperature	5.0 keV	7.0×10^{18}m^{-3}
High Confinement	1.1 keV	6.5×10^{19} m^{-3}
$\tau_E = 0.36$ s, $nT\tau_E = 2.2 \times 10^{19}$ keV m^{-3}, $P_{abs} = 2$ MW,		
Maximum Stored Energy	$W_p = 1.12$ MJ	
Highest Beta	$<\beta> = 3.2$ % at $B = 0.5$ T	
Maximum Density	1.5×10^{20} m^{-3}	

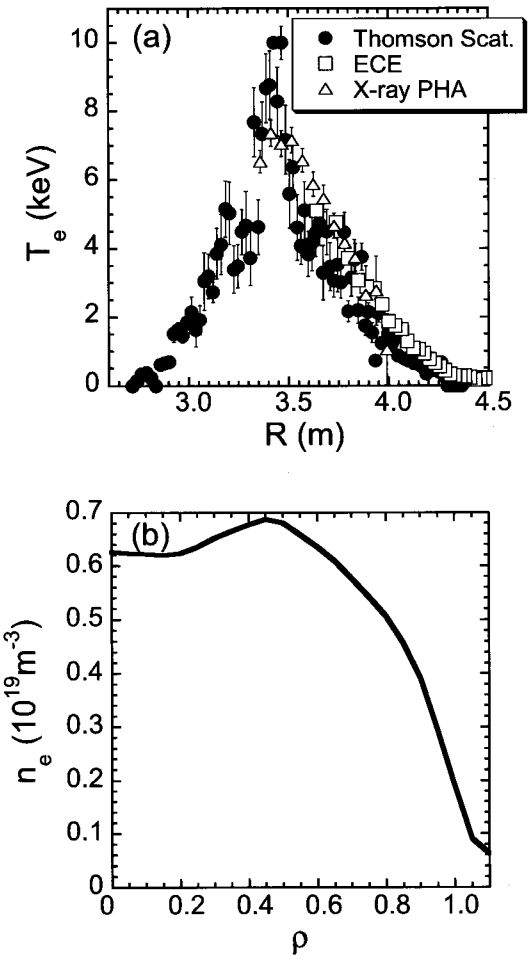

Fig. 3 Achieved highest electron temperature. (a) Electron temperature profile measured by Thomson scattering (solid circles), ECE (open squares), and X-ray PHA (open triangles). (b) Density profile reconstructed from the line density measurement by a multi-channel FIR interferometer.

3. Global Energy Confinement and MHD Stability

The energy confinement times in the configuration with the inward shifted magnetic axis ($R_{ax} = 3.6$ m) are consistent with the ISS95 scaling [10] with an enhancement factor of ~1.5 and are comparable to those in ELMy H-mode discharges (tokamaks) [11]. The characteristics of the energy confinement time is gyro-Bohm. It is a factor of 2 higher than those of smaller heliotron devices such as CHS, Heliotron E, ATF. This enhancement is attributed to high edge temperature due to monotonically decreasing heat conduction coefficient towards the edge, which has not observed in medium-sized experiments [12,13]. Dependence of the energy confinement on the magnetic configurations particularly the position of the magnetic axis was studied [14]. Numerical calculation shows that the configuration with the inward shifted magnetic axis ($R_{ax} = 3.5$–3.6 m) has the best particle orbit properties, i.e., deviation of the deeply trapped particle orbit from the magnetic surface is minimum and the deviation becomes larger with increasing R_{ax} [14,15]. This is important because suppression of the neoclassical transport as well as the anomalous transport are required for high plasma performance. Figure 4(a) shows that the enhancement factor over the ISS95 scaling is found to be sensitive to the variation in the magnetic axis (R_{ax}) [8]. The

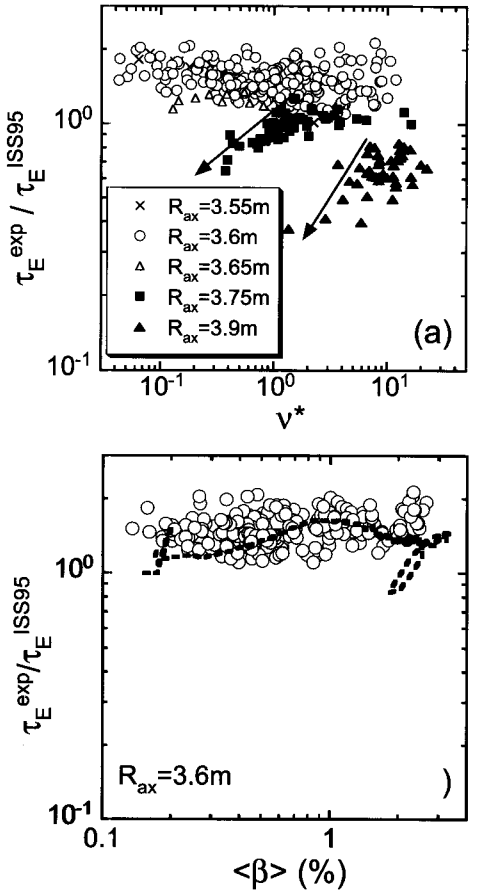

Fig. 4 Confinement enhancement factor over ISS95 as a function of (a) collisionality and (b) volume averaged beta. The dotted line is the time trace of a single discharge reaching <β> of 3%.

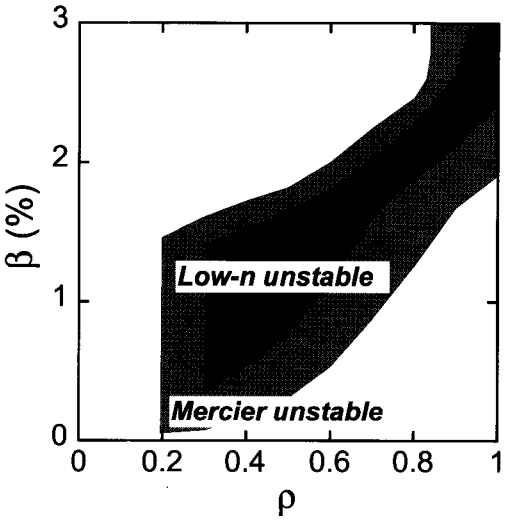

Fig. 5 Theoretical MHD stability diagram on the plane of beta and the minor radius. The parabolic pressure profile is assumed.

confinement is improved at R_{ax} = 3.55–3.6 m and decreases with increasing R_{ax}. For R_{ax} = 3.9 m, it is as small as 0.6. Furthermore, strong deterioration of the confinement occurs for R_{ax} = 3.75 and 3.9 m when the plasma becomes collisionless ($\nu^* < 1$, ν^* is defined by the transition point of the banana and plateau regimes.) This is attributed to the neoclassical transport. For the inward shifted configuration with low neoclassical transport, the enhancement factor is independent of ν^* and hence the anomalous transport dominates over the neoclassical transport.

The average <β> of ~ 3 % at B = 0.5 T has been achieved and the <β> value is limited by the available heating power in the present experimental condition [8]. It is realized in the inward shifted configuration (R_{ax} ~ 3.60 m), in which magnetic hill exists in the entire region. With increasing <β>, low n coherent modes (n/m=1/2, 1/1 and 3/2) appear [16]. The mode (n/m=1/2) disappears when <β> exceeds 2.3 %. The pressure profile is flat in the core and high-pressure gradient exists in the edge. The observed pressure gradient ($d\beta/dr$) exceeds the Mercier stability limit in nearly a half of the plasma-confining region. Figure 5 shows the theoretical stability diagram. At ρ = 0.9 (ι= 1.0), it becomes Mercier unstable when <β> exceeds 1.8 % and is even unstable to low n mode when <β> exceeds 2.1 %. On the other hand, at ρ = 0.5 (ι= 0.5), the observed pressure profile is unstable up to <β> = 2 %. But it becomes stable when <β> increases further (the second stability). The observed magnetic fluctuations, which generally increase with <β> do not lead to any serious MHD phenomenon which degrades the confinement time (see Fig. 4(b)). The drop seen in the time trace of high-β discharge in Fig. 4(b) is due to a temporal cooling by pellet injection and not due to any instability. It is significant and very encouraging that the MHD stability is demonstrated in the inward shifted configuration, which has good transport properties.

4. Internal Transport Barrier (ITB) Formation

Enhancement of the confinement is the major research efforts in the LHD program. When the ECRH power is absorbed in the central region (ρ < 0.2) of NBI heated plasmas, ITB-like temperature profile, which is similar to that in CHS [17] has been observed, as shown in Fig. 6(a). The theoretical calculation based on neoclassical transport suggests that existence of electron-root in the core is related to formation of ITB through enhanced radial electric field [18]. This ITB-like profile is obtained when the ECRH power exceeds a

threshold value (see Fig. 6(b)). This threshold increases with increasing density and decreasing NBI power. The decay time of the central electron temperature after turning-off of ECRH power is significantly slower in the case with ITB than without ITB. This suggests the transport improvement inside ITB, which is an encouraging sign of confinement enhancement.

5. Long Pulse Discharges

Demonstration of steady-state plasma with high performance is one of the most challenging issues. Such investigation is particularly appropriate for the research program in LHD which employs superconducting coils [19,20]. The NBI (0.5 MW) heated plasma was sustained up to 80 s (see Fig. 7(a))and the ICRF (0.4 MW) heated plasma with the discharge duration of 2 minutes (see Fig. 7(b)) is achieved. In both discharges with helium gas puffing, the electron densities are kept to be around 1×10^{19}m^{-3} and the temperatures were one to two keV during the discharge. It should be pointed out that recycling is not saturated in this 2-minute discharge. The longer discharge is required to verify necessity of an active particle control. The radiation power is less than 25 % of the input power and there was no sign of impurity accumulation. As to the operational density limit in long pulse discharges, high-density plasma with 6.7×10^{19}m^{-3} is sustained for 10 s with a NBI power of 2 MW. The global energy confinement characteristics of long-duration plasmas are almost the same as those in short-pulse discharges [21].

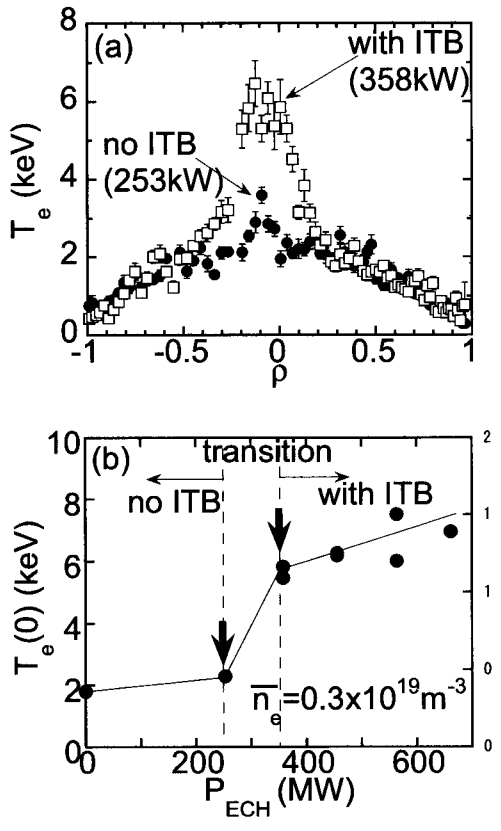

Fig. 6 Observation ITB-like structure. (a) Electron temperature profile with high and low heating power across the transition. (b) Dependence of the central electron temperature on heating power. Arrows correspond to the cases shown in (a).

6. Discussions and Future Prospect

The experiments in LHD have greatly extended the envelope of study on net current-free plasmas in these three and a half years. Significant progress can be seen in achievement of the representative plasma parameters (W_p = 1.12 MJ, $T_e(0)$ = 10 keV, $T_i(0)$ = 5keV, β = 3.2 %). The energy confinement time of LHD plasmas is comparable to that of the ELMy H-mode plasmas in tokamaks with q=4.5 from the aspect of the scaling law [22]. The most important finding is that good MHD stability and good transport are compatible in the inward shifted configuration (R_{ax} = 3.6m). This finding gives a perspective of the heliotron line a breakthrough. The inward shifted configuration has magnetic hill geometry and thus was predicted to be MHD unstable by ideal

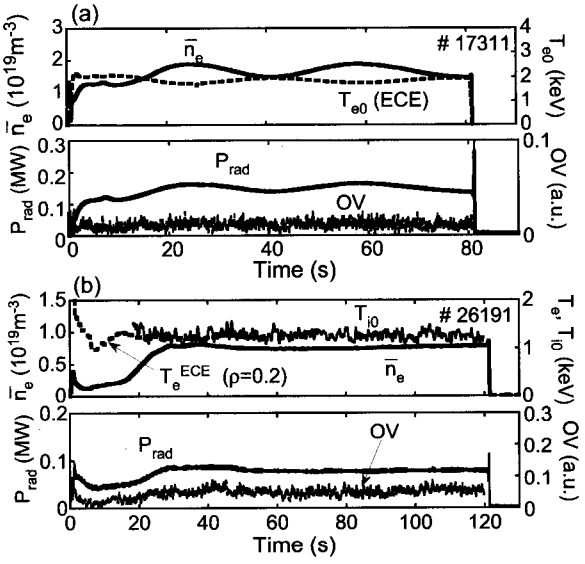

Fig. 7 Typical wave forms of long-pulse discharges. (a) NBI heated plasma. Slow undulation is due to intentional density control not due to spontaneous behavior of plasma. (b) ICRH plasma.

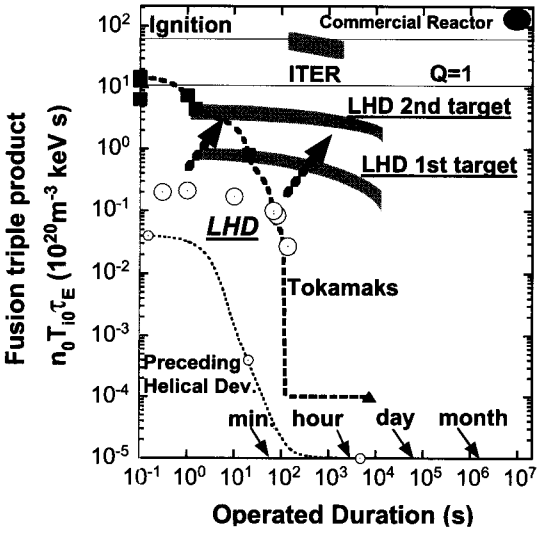

Fig. 8 Diagram of development of fusion plasmas on the plane of the fusion triple product and the operated duration.

linear MHD stability theory. But plasma is stable at least up to β = 3 %. The geometrical optimization of neoclassical transport by the inward shift of the magnetic axis is quite successful, however, the mechanism of suppression of anomalous transport due to the inward shift is still an open question. With central deposition of ECRH power, the ITB shape profiles are seen, providing a hope for further confinement improvement. The other important achievements and observations are (i) a long pulse discharge with duration time of 2 minutes (80 seconds) has been achieved with 0.4 MW ICRH (0.5 MW NBI) power, respectively. (ii) The external imposed island (n/m=1/1) is suppressed with collionless finite beta plasmas. (iii) ICRF heating (minority ion heating) has been very successful and the heating efficiency is comparable to that of NBI heating [23-25]. (iv) The transition from ion root to electron root has been observed [26]. (v) The divertor is very effective in preventing impurity contamination. Fine field structure in the divertor region has been confirmed by measuring the divertor plasma by electrostatic probes [27,28]. (vi) Pellet injection is very helpful in raising the operational density limit and achieving high stored energy [29].

Figure 8 shows the operational regime on the plane of the fusion triple product and operated duration. The final goal is clearly defined and this figure indicates that steady state operation is the most challenging issue. The 1st target is possible by maximizing the present experimental capability. The 2nd target is held up with reasonable upgrade of the machine. LHD is surpassing the existing tokamak experiments in terms of operated duration with significant plasma parameters.

References

[1] A. Iiyoshi *et al.*, Fusion Technol. **17**, 169 (1990).
[2] A. Iiyoshi *et al.*, Nucl. Fusion **39**, 1245 (1999).
[3] O. Motojima *et al.*, Phys. Plasma **6**, 1843 (1999).
[4] N. Ohyabu *et al.*, Phys. Plasmas **7**, 1802 (2000).
[5] Kawahata *et al.*, Plasma Phys. Control. Fusion **42**, B51 (2000).
[6] M. Fujiwara *et al.*, Nucl. Fusion **41**, 1355 (2001).
[7] A. Komori *et al.*, Phys. Plasmas **8**, 2002 (2001).
[8] H. Yamada *et al.*, *to appear in* Plasma Phys. Control. Fusion.
[9] O. Kaneko *et al.*, Nucl. Fusion **39**, 1087 (1999).
[10] U. Stroth *et al.*, Nucl. Fusion **36**, 1063 (1996).
[11] H. Yamada *et al.*, Nucl. Fusion **41**, 901 (2001).
[12] N. Ohyabu *et al.*, Phys. Rev. Lett. **84**, 103 (2000).
[13] H. Yamada *et al.*, Phys. Rev. Lett. **84**, 1216 (2000).
[14] S. Murakami *et al.*, *to appear in* Nuclear Fusion.
[15] H.E. Mynick, T.K. Chu and A.H. Boozer, Phys. Rev. Lett. **48**, 322 (1982).
[16] S. Sakakibara et al., Nucl. Fusion **41**, 1177 (2001).
[17] A. Fujisawa *et al.*, Phys. Rev. Lett. **82**, 2669 (1999).
[18] K. Itoh *et al.*, J.Phys.Soc. Jpn. **70**, 1575 (2001).
[19] N. Noda *et al.*, Nucl. Fusion **41**, 779 (2001).
[20] M. Fujiwara *et al.*, Nucl. Fusion **40**, 1157 (2000).
[21] Y. Nakamura *et al.*, J. Nucl. Mater. **290-293**, 1040 (2001).
[22] H.Yamada *et al.*, Plasma Phys. Control. Fusion **44**, A245 (2002).
[23] T. Mutoh *et al.*, Phys. Rev. Lett. **84**, 4530 (2000).
[24] T. Watari *et al.*, Nucl. Fusion **41**, 325 (2001).
[25] R. Kumazawa *et al.*, Phys. Plasmas **8**, 2139 (2001).
[26] K. Ida *et al.*, Phys Rev. Lett. **86**, 5297 (2001).
[27] T. Morisaki *et al.*, Contrib. Plasma Phys. **40**, 266 (2000).
[28] S. Masuzaki *et al.*, J. Nucl. Mater. **290-293**, 12 (2001).
[29] R. Sakamoto *et al.*, Nucl. Fusion. **41**, 381 (2001).